Chapter 2
Investigation of Cutting Edge Radius Effect in Macro-machining and Micro-machining

Juri Saedon, Noor Aniza Norrdin, Mohd Azman Yahaya, Mohd Shahir Kasim and NorHafiez Mohamad Nor

Abstract Chip formation is a dynamic process that is often nonlinear in nature. A chip may not form when the depth of cut is less than a minimum chip thickness. This paper presents an investigation of cutting edge radius effect in macro- and micro-machining of AISI D2 steel via simulation using ABAQUS software. Through the arbitrary Lagrangian–Eulerian FE modeling approach, the chip growth, chip formation, and cutting force were investigated under three criteria such as $a/r < 1$, $a/r > 1$, and $a/r = 1$. The results from this simulation can provide useful information for choosing reasonable cutting edge to improve surface integrity and prolong cutting tool life in macro- and micro-milling operation. It is found that the chip is formed at $a/r > 1$ while material extrusion performed under $a/r < 1$. The investigation on the cutting force found that value of a/r ratios greatly affects the cutting force. The cutting mechanism in micro-milling is similar to macro-milling due to the process undergoes both ploughing and shearing mechanism.

Keywords Chip formation · FEA · Cutting edge radius · Minimum chip thickness

---

J. Saedon · N.A. Norrdin (✉) · M.A. Yahaya · N. Mohamad Nor
Faculty of Mechanical Engineering, Universiti Teknologi MARA,
Shah Alam, Selangor, Malaysia
e-mail: nr.aniza@yahoo.com

J. Saedon
e-mail: juri41@yahoo.com

M.A. Yahaya
e-mail: yahayama@yahoo.com

N. Mohamad Nor
e-mail: norhafiez@yahoo.com

M.S. Kasim
Faculty of Manufacturing Engineering, Universiti Teknikal Malaysia,
Durian Tunggal, Malaysia
e-mail: shahir@utem.edu.my

N.A. Yacob et al. (eds.), *Regional Conference on Science, Technology and Social Sciences (RCSTSS 2014)*, DOI 10.1007/978-981-10-0534-3_2

1 Introduction

AISI D2 hardened tool steel is a high chromium, high carbon, tool and die steel with hardness in the range 54–62 HRC used for cold working operations. It has a high strength, very high resistance to cracking, and high resistance to softening and wear. Most recently, there are large amounts of work on hardened tool steel material toward the implementation of replication technology for mass production of miniaturization parts and components. But machining of hardened tool steel materials in manufacturing of moulds for replication technologies are mostly challenging. This is due to unpredictable tool life, premature of tool failure and differences in process mechanisms compared to macro-milling. Therefore, a good finite element model (FEM) simulation of machining AISI D2 would be very useful to optimize the machining process and led to reduce its costs, machining time saving, improved the quality and quantity.

In order to present the main differences in chip formation due to the scaling-down from macro- to micro-milling, a short review of the current state of the art in chip formation and minimum chip thickness in micro-milling is carried out. Then the FEM developed is presented and the results will be comparing to those found in the literature. The chip formation mechanism was studied quantitatively via FEM approach.

2 Comparison Between Micro-milling and Macro-milling

The effect of cutting edge radius was the significant contrast in cutting process between macro- and micro-machining methods. In macro-cutting, the cutting edge radius of carbides tools might be considered to be sharp as the uncut chip thickness is significantly larger than the cutting edge radius, see Fig. 1a. However, in micro-cutting, the uncut chip thickness is frequently smaller than the cutting edge

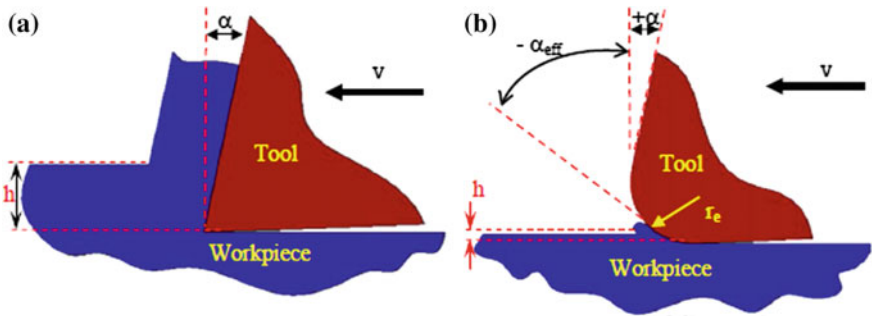

Fig. 1 Effect of cutting edge radius to chip thickness in macro-cutting (**a**) and micro-cutting (**b**) (Saedon et al. 2013)

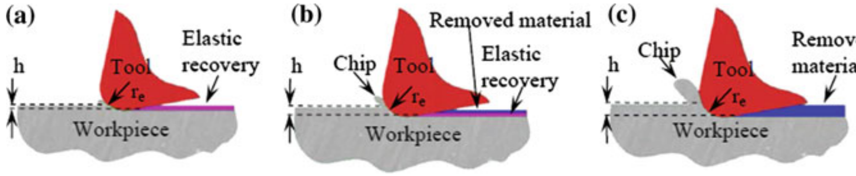

Fig. 2 Chip formation with respect to chip thickness in micro machining based on Saedon et al. (2013). **a** $h < h_{min}$, **b** $h \cong h_{min}$, **c** $h > h_{min}$

radius and the chip is structures in the zone of the cutting edge radius, see Fig. 1b. Thus, a profoundly negative rake angle exists and the apparent relative bluntness of the tool increases the specific cutting forces (Saedon 2011).

The minimum chip thickness h_{min} is characterized as the minimum undeformed thickness of the chip removed from a work surface at a cutting edge. In macro-machining, the depth of cut is generally greater than the cutting tool edge radius, and it is assumed that the cutting tools totally remove the surface of the workpiece and generate the chips. It is different in micro-machining where, the small depth of cut compared to the edge radius of the tool causes a large negative rake edge. The consequence of this is a process, which might be dominated more by rubbing and compression instead of cutting. This phenomenon causes a rough surface roughness and elastic recovery of the workpiece, increasing the possibilities tool damages to happen. Three different cases happen in micro-chip formation, as shown in Fig. 2.

At the point when the uncut chip thickness, a, is less than a critical minimum chip thickness, h_{min}, elastic deformation happens and the cutter does not remove any chip as shown in Fig. 2a. When the uncut chip thickness comes near to the minimum chip thickness, h_{min}, chips are form by shearing of the workpiece, with some elastic deformation even at this time still happening as shown in Fig. 2b. However when the uncut chip thickness increases further than the minimum chip thickness, h_{min}, the elastic deformation become lessen and chip is removed as shown in Fig. 2c. The minimum chip thickness phenomena can contribute to the increase of the cutting force due to the rising of slipping forces and ploughing of the machined surface.

3 Methodology—Finite Element Modelling (FEM)

In this study, ABAQUS/EXPLICIT software was used in macro-milling and micro-milling of AISI D2 tool steel. A two dimensional explicit dynamic algorithm coupled with Arbitrary Lagrangian–Eulerian (ALE) as a solution method was developed. The workpiece and cutter material for the both macro- and micro-scale model is AISI D2 tool steel and tungsten carbide, respectively. The workpiece is modelled as a rectangular block with a dimension of 30 mm long 15 mm thick for

Table 1 Machining parameter modelling

Machining scale	Cutting parameters				
	Angles cutter (deg)		Cutting speed, V_c (m/min)	Cutting depth, d	Feed rates, f (mm/tooth)
	Rake γ	Clearance α			
Macro scale	5	5	100	1.5	0.2
Micro scale	5	5	100	3	0.2

macro-scale model and while for micro-scale model is 50 μm long and 15 μm thick. The machining parameters: cutting speed, V_c (m/min), cutting depth, d, and feed rates, f, (mm/tooth) are shown in Table 1.

The cutting tool geometry is treated as perfectly rigid solids while workpiece is assumed to be deformable. The simulation was carried out with positive 5° rake angle and 5° clearance angle at different cutting tool edge radius, $r = 0.5$, 1.5, 2.5, and 5.7 mm for macro scale and $r = 1$, 3, 5 and 8 μm for micro scale. Various a/r ratios have been considered in order to study the influence of the cutting tool edge radius on the chip formation process. Four different cases have been simulated from $a/r = 3$, $a/r = 1$, $a/r = 0.6$ and $a/r = 0.2$. The workpiece is assumed homogeneous and plastic flow behaviour around the cutting edge was governed by Johnson–Cook material model of Eq. (1).

$$\sigma = (A + B\,\varepsilon_\rho^n)\,(1 + C\ln(\acute{\varepsilon}/\acute{\varepsilon}_o))\,(1 - (T - T_\gamma/T_m - T_\gamma)^m) \quad (1)$$

where σ is flow stress, ε_ρ and ε are strain and strain rate, ε_o is the reference stain rate (1/s) and n, m, A, B and C are constant parameters for Johnson–Cook material model as shown in Table 2.

Table 2 FEM properties

Workpiece properties (AISI D2)	
Yield strength (Mpa)	1776
Hardening modulus (Mpa)	904
Strain rate sensitivity	0.012
Thermal softening coefficient	3.38
Hardening coefficient	0.312
Reference strain rate	1
Melting temperature (°)	1460
Density (kg m^{-3})	7750
Elastic modulus (Gpa)	200
Poisson's ratio	0.3
Specific heat (J kg^{-1} K^{-1})	485
Thermal expansion(10^{-6} °C)	10.4
Thermal conductivity (W/m K)	21

Total mesh generated for the micro scale model was 4791 of elements, while 4955 nodes have been set as the region of the chip formation analysis. It is different to the macro scale model where there was 5213 of elements and 5061 nodes. Figure 3 shows meshed and the predefined boundary conditions where the reference point was set at the cutting tool tip. The bottom and left side of the workpiece are fixed in vertical and horizontal direction. The displacement of tool for *y*-axis and rotation of tool for both *x*-axis and *y*-axis are fixed but the tool is permitted to move horizontally in *x*-axis at a cutting speed of 100 m/min.

The study can estimate the chip growth, chip formation, and cutting force at several tool radiuses, *r* while the cutting speed, V_c (m/min), feed rates, *f* (mm/tooth) and depth of cut, *d* were held constant. The values were estimated by using FEM as shown in Table 3.

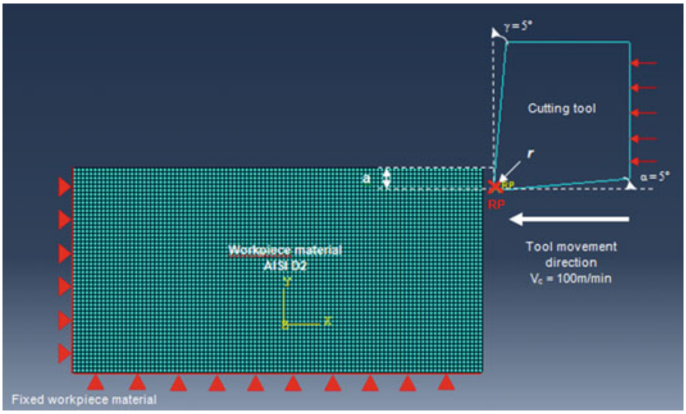

Fig. 3 FEM model with predefined boundary condition

Table 3 Machining process performed at several edge radiuses

Machining scale	Simulation numbers	Edge radiuses, *r* (mm, µm)	Cutting parameters		
			Cutting speed, V_c (m/min)	Cutting depth, *d* (mm)	Feed rates, *f* (mm/tooth)
Macro scale	S1	0.5	100	1.5	0.2
	S2	1.5			
	S3	2.5			
	S4	5.7			
Micro scale	S5	1	100	3	0.2
	S6	3			
	S7	5			
	S8	8			

4 Results and Discussion

Chip Formation

Figures 4, 5, 6, and 7 shows chip formation and material deformation for various *a*/*r* ratios values. A chip certainly formed when *a*/*r* = 3 and 1, however it is not for *a*/*r* = 0.6 and 0.2 for both macro- and micro-scale model. Therefore, it is possible to give judgment on the existence of a chip. The presence of a saw-tooth chip when *a*/*r* = 3, as observed in Fig. 4. This kind of chip is not found any more for smaller simulated *a*/*r* values as shown in Figs. 6 and 7.

A primary shear zone is able to be seen on Von Mises stress contours when *a*/*r* = 3, as in micro- and macro-cutting with a sharp tool. Chip forms easily within this area. As the material reaches its yield point, chips will forms from the parent

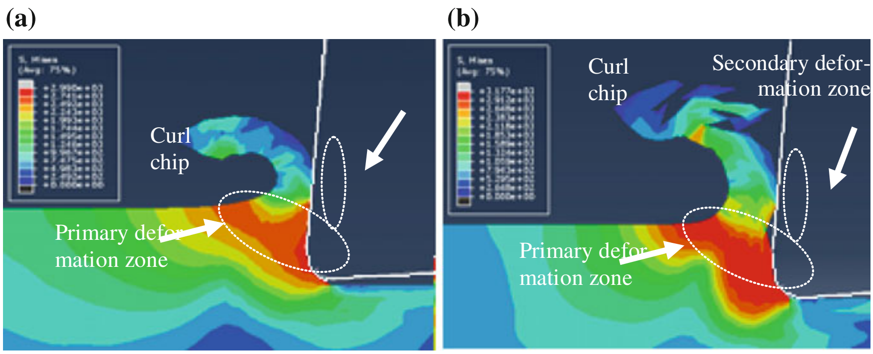

Fig. 4 Von Mises stress contours (10^3 Pa) during chip formation **a** macro-cutting and **b** micro-cutting at *a*/*r* = 3

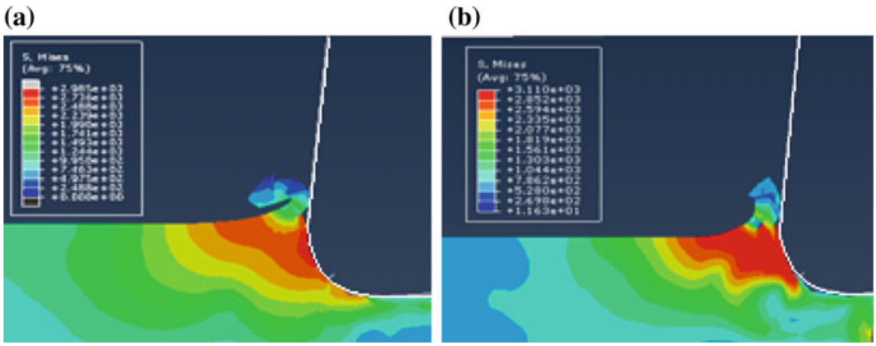

Fig. 5 Von Mises stress contours (10^3 Pa) during chip formation **a** macro-cutting and **b** micro-cutting at *a*/*r* = 1

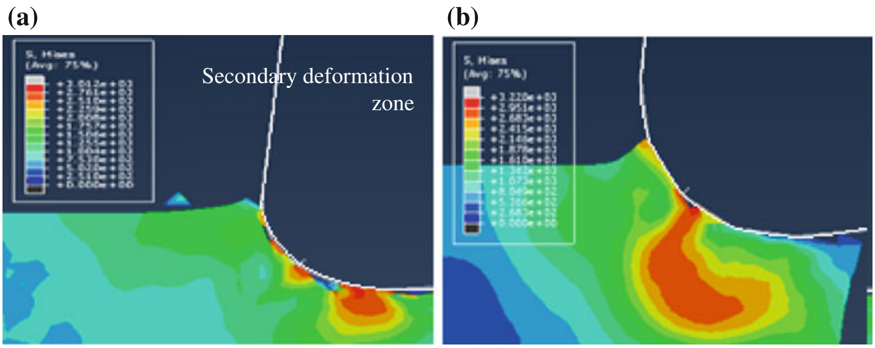

Fig. 6 Von Mises stress contours (10^3 Pa) during chip formation **a** macro-cutting and **b** micro-cutting at $a/r = 0.6$

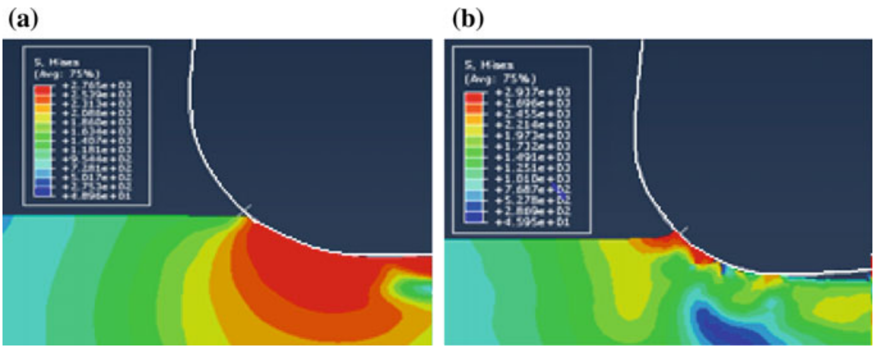

Fig. 7 Von Mises stress contours (10^3 Pa) during chip formation **a** macro-cutting and **b** micro-cutting at $a/r = 0.3$

material and slides along the primary shear plane, pushing material ahead of the cutting tool as in Fig. 4. A secondary shear zone occurs along the face of the cutting tool. In this zone, the friction raises temperature when the chip slides up the face of the cutting tool.

The more the a/r ratio decreases, the more the primary shear zone fades and it cannot be distinguish any longer from the $a/r = 0.2$ value. When $a/r < 1$, a primary shear zone can still be seen but the stress value seems to be smaller, also there are no secondary deformation zone found due to the reason that no chip is formed.

The results for micro-cutting are similar to those ALE model presented by Woon et al. (2008). The cutting tool edge radius and also the a/r value has great influence on the chip formation in micro-cutting. When looking to Figs. 4, 5, 6, and 7 the cutting mechanism in micro-milling is similar to macro-milling due to the reason that process undergoes both ploughing and shearing mechanism.

Cutting Force

Figures 8 and 9 show the cutting and feed forces for a 1.5 mm and 3 µm depth on cut. The cutting force and feed directions are determined at the reference point (RP). The cutting force is greater than the feed force in micro-cutting, which also observed in macro-cutting. The fluctuation evolution can be seen, as expected due to the saw-toothed chip where the slipping plane occurs and the up and down in the forces is observed.

Figure 10 represents the ratio between feed and cutting forces for the eight *a*/*r* simulated ratios, four ratios for macro-cutting and four ratios for micro-cutting. From the graph obtained, the more the *a*/*r* ratio decreases, the more the forces ratio (feed/cutting force) increases. This is due to the feed force becomes greater than the cutting force when the *a*/*r* ratio value becomes smaller. It is similar to both macro- and micro-cutting. These observations are similar to those made experimentally by Liu et al. (2012). Afazov et al. (2010) also mentioned that the forces at small uncut chip thickness are mainly affected by the tool radius. Therefore, it is possible to give

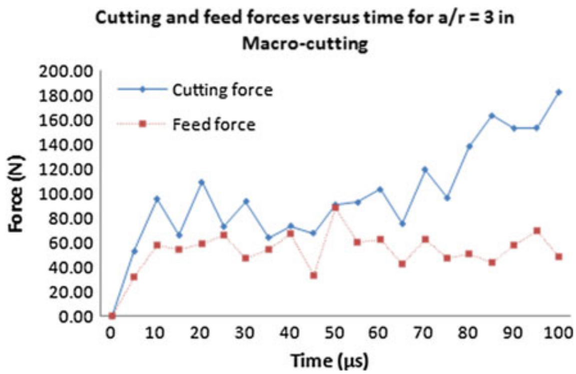

Fig. 8 Forces during macro-cutting when *a*/*r* = 3

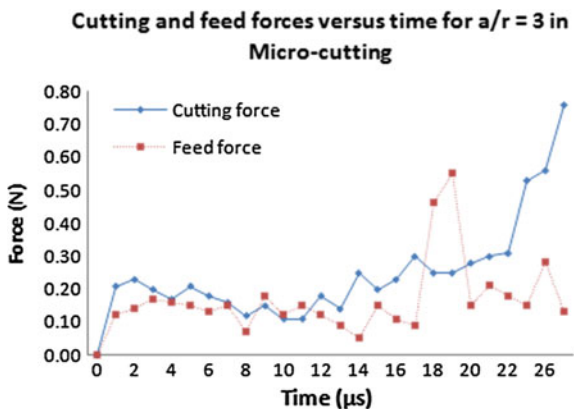

Fig. 9 Forces during micro-cutting when *a*/*r* = 3

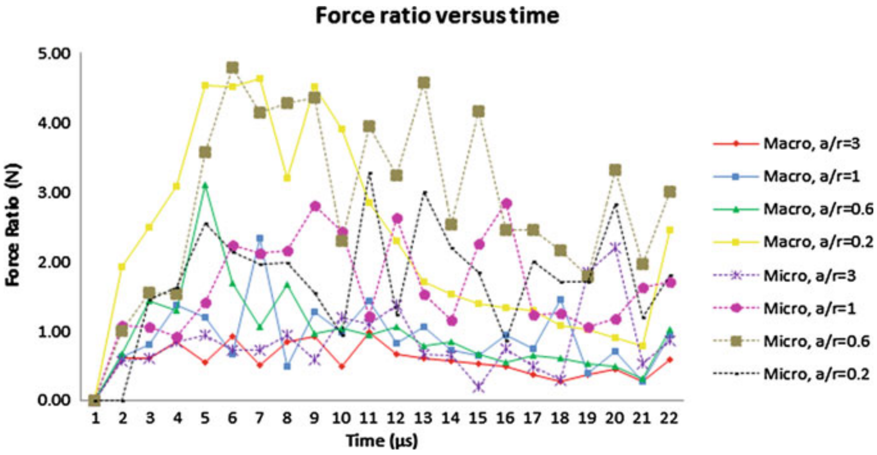

Fig. 10 Forces ratio during macro- and micro-cutting various *a*/*r*

judgment on the smaller value of *a*/*r* ratio creates a negative rake angle between the cutting tool and the workpiece which affects the chip formation and the cutting force, respectively.

5 Conclusion

In this work, the chip growth, chip formation and cutting force in the macro- and micro-machining process was investigated. The chip formation mechanism was studied quantitatively via FEM approach. Some important results were found as follows:

1. The transition from macro- to micro-cutting leads to some difference in chip morphologies when compared to orthogonal cutting. From the results, it is showed that the cutting mechanism in micro-milling is similar to macro-milling due to the process undergoes both ploughing and shearing mechanism. The macro- and micro cutting model showed that the chip formed perfectly at $a/r > 1$ and $a/r = 1$ while material extrusion performed under $a/r < 1$ ratio.
2. There are two zones for plastic deformation such as primary shear zone and secondary shear zone. From the observation, the primary shear zone appears to be most predominant and there are no secondary shear zone was found under $a/r < 1$ ratio due to no chip formed.
3. The smaller value of *a*/*r* ratio creates a negative rake angle between the cutting tool and the workpiece which affects the chip formation and the cutting force, respectively.

References

Afazov SM, Ratchev SM, Segal J (2010) Modelling and simulation of micro-milling cutting forces. J Mater Process Technol 210(15):2154–2162. http://linkinghub.elsevier.com/retrieve/pii/S0924013610002335. Accessed 24 March 2014

Liu HT et al (2012) Finite element simulation and experimental research on micro-milling process of titanium alloy. Key Eng Mater 522:245–248. http://www.scientific.net/KEM.522.245. Accessed 31 March 2014

Saedon J (2011) Micromilling of hardened (62 HRC) AISI D2 cold work

Saedon JB et al (2013) Influence of cutting edge radius in micromachining AISI D2. Appl Mech Mater 393:253–258. http://www.scientific.net/AMM.393.253. Accessed 28 April 2014

Woon KS et al (2008) Investigations of tool edge radius effect in micromachining: a FEM simulation approach. J Mater Process Technol 195(1–3):204–211. http://www.sciencedirect.com/science/article/pii/S0924013607005031. Accessed 30 April 2014

http://www.springer.com/978-981-10-0532-9

Regional Conference on Science, Technology and
Social Sciences (RCSTSS 2014)
Science and Technology
Yacob, N.A.; Mohamed, M.; Megat Hanafiah, M.A.K.
(Eds.)
2016, XVI, 649 p. 244 illus. in color., Hardcover
ISBN: 978-981-10-0532-9